HHS Public Access

Author manuscript

Neuroscience. Author manuscript; available in PMC 2023 August 21.

Published in final edited form as:

Neuroscience. 2022 August 21; 498: 85–92. doi:10.1016/j.neuroscience.2022.06.030.

Reducing Taperin Expression Restores Hearing in *Grxcr2* Mutant Mice

Chang Liu[1], **Na Luo**[1], **Bo Zhao**[1,*]

[1]Department of Otolaryngology-Head and Neck Surgery, Indiana University School of Medicine, Indianapolis, IN 46202, USA

Abstract

Recessive mutations in GRXCR2 cause deafness in both humans and mice. In *Grxcr2* null hair cells, the sensory receptors for sound in the inner ear, stereocilia are disorganized. Reducing the expression of taperin, a protein that interacts with GRXCR2 at the base of stereocilia, corrects the morphological defects of stereocilia and restores hearing in *Grxcr2* null mice. To further validate this finding, this study generated two novel *taperin* mutant mouse lines that exhibit progressive hearing loss. Then *Grxcr2* null mice were crossed with one of these *taperin* mutant mice. The following morphological analysis revealed that reducing taperin expression indeed corrected stereocilia morphological abnormalities in *Grxcr2* null mice. Functional analysis further confirmed that reducing taperin expression partially restored hearing in *Grxcr2* null mice.

Keywords

GRXCR2; taperin; stereocilia; deafness; hearing loss

INTRODUCTION:

Around 466 million individuals globally, or 6% of the population, suffer from hearing loss (Olusanya et al., 2019). The most frequent type of permanent hearing loss is sensorineural hearing loss. It is typically caused by defects in cochlear hair cells, the inner ear sensory receptors that convert mechanical sound vibrations into electrical signals. Hair cells are vulnerable to genetic mutations, which are responsible for roughly 80% of prelingual deafness (Shearer et al., 1993). By 2011, 135 loci had been identified for human monogenic types of deafness (Richardson et al., 2011). Over 70 of the affected genes have been

*Corresponding author: Bo Zhao, Department of Otolaryngology Head & Neck Surgery, Indiana University School of Medicine, Indianapolis, IN 46202, USA, zhaozb@iu.edu, T: 317-274-4918.

AUTHOR CONTRIBUTIONS

Methodology, C.L., N.L. and B.Z.; Investigation, C.L., N.L. and B.Z; Writing, C.L. and B.Z; Conceptualization and Supervision, B.Z..

CONFLICT OF INTEREST

All authors declare no competing interests.

identified thus far, and a significant proportion of these genes are abundantly expressed in hair cells and are essential for hair cell morphogenesis.

Hair bundles, specialized subcellular organelles protruding from the apical surfaces of hair cells, are composed of several rows of organized stereocilia (Barr-Gillespie, 2015; Zhao and Muller, 2015). The core of stereocilia is composed of a paracrystalline array of parallel actin filaments, which are oriented with fast-growing barbed ends at the tips of stereocilia and pointed ends at the base (Drummond et al., 2015; Narayanan et al., 2015). At the base of stereocilia, a few actin filaments extending into the cuticular plate form rootlets that provide rigidity to stereocilia (Kitajiri et al., 2010). Taperin, mutations of which cause the autosomal recessive nonsyndromic hearing loss type 79 (DFNB79), localizes at the base of stereocilia (Li et al., 2010; Rehman et al., 2010). Notably, taperin is able to regulate the actin cytoskeleton, as evidenced by the formation of rodlike actin filaments in COS7 cells and extraordinary stereocilia growth in hair cells when it is overexpressed (Liu et al., 2018). GRXCR2, another deafness-related protein, interacts with taperin and regulates its localization at the base of stereocilia (Avenarius et al., 2018; Imtiaz et al., 2014; Liu et al., 2018; Wonkam et al., 2021). Hair cells lacking GRXCR2 have disorganized stereocilia due to the mislocalization of taperin. Reducing taperin expression in *Grxcr2* null mutant mice rescues the morphological defects of stereocilia and partially restores hearing in *Grxcr2* null mice (Liu et al., 2018).

To further validate that GRXCR2 is essential for the morphogenesis of stereocilia via regulating taperin localization, we generated two novel *taperin* mutant mouse lines with progressive hearing loss. Then, we crossed *Grxcr2* null mice with one of these *taperin* mutant mice. Morphology of stereocilia was analyzed using whole mount immunostaining and scanning electron microscopy. Auditory functions were evaluated by measuring the auditory brainstem responses (ABRs). Our results demonstrate that reducing taperin expression does indeed correct stereocilia morphological defects and partially restore hearing in *Grxcr2* null mutant mice.

EXPERIMENTAL PROCEDURES:

Animal Models and Animal Care

Grxcr2$^{-/-}$ mouse (previously referred to as the *Grxcr2*$^{D46/D46}$ mouse) has been described previously (Liu et al., 2018). *taperin*$^{D23/D23}$ and *taperin*$^{D11/D11}$ mice were generated using CRISPR/Cas9 technology. In brief, the sequences 5’-GGATCTGGAGCGGCGCCGGATGG -3’ and 5’- CGACGGCACTGCCGGCCCCGGGG -3’ were chosen as the sgRNA target genomic DNA sequences. Chimeric guide RNAs were synthesized *in vitro* using the published protocol (Yang et al., 2014). One-cell embryos were microinjected by the genomics facility at The Scripps Research Institute. The founder mice were back-crossed with C57BL/6J mice for two generations. The following primers were used to genotype *taperin*$^{D23/D23}$ and *taperin*$^{D11/D11}$ mice: 5’-CTGGAAACGGGAGATCCTTG -3’ and 5’- GAAGCCTGGCGCTGACTC -3’. All animal experiments were approved by Institutional Animal Care and Use Committee of The Scripps Research Institute and Indiana University School of Medicine. Male and female mice were used in our experiment. No difference in auditory function was observed between the sexes.

Whole Mount Immunostaining

Staining of the cochlear whole mount was performed as described (Li et al., 2021; Liu et al., 2018). In brief, the organ of Corti was dissected and fixed in 4% PFA in Hank's Balanced Salt Solution (HBSS) for 20 min. Samples were blocked for 20 min at room temperature in HBSS containing 5% bovine serum albumin (BSA), 1% goat serum and 0.5% Triton X-100, followed by overnight incubation at 4°C with primary antibodies. After being washed in HBSS, samples were incubated with secondary antibodies at room temperature for 2 hours. ProLong® Antifade Reagents (Invitrogen) were used to mount tissues. Stacked images (Z step, ~0.17 μm) were then captured using a 100 X objective (HCX PL APO 100x/1.40-0.70 OIL) on a deconvolution microscope (Leica). Following that, images were deconvoluted using blind deconvolution method.

To raise antibodies against taperin, we covalently bonded a peptide (NLTPASQNDLSDFRSEPALYF -C) derived from the primary sequence of mouse taperin to KLH and injected it into New Zealand rabbits (Covance). Then, antibodies were obtained using affinity purification. Other primary antibodies were as follows: anti-GRXCR2 (Cat# HPA059421, Sigma) and anti-taperin (Cat# HPA020899, Sigma). Additional reagents were: Alexa Fluor 488 phalloidin (ThermoFisher Scientific), Alexa Fluor 568-phalloidin (ThermoFisher Scientific) and Alexa Fluor 488 goat anti-rabbit (ThermoFisher Scientific).

RNA Isolation and Reverse Transcription Polymerase Chain Reaction (RT-PCR)

The organ of Corti were dissected from P7 *taperin*$^{D11/D11}$ and *Grxcr2*$^{-/-}$ *taperin*$^{D23/D23}$ mice. RNA was isolated using RNeasy Kit (Qiagen) and then reverse transcribed using SuperScript III reverse transcriptase (Life technologies). Then Platinum™ SuperFi™ DNA Polymerase (Life technologies), and primers 5'-GCTAGTCGACGGAAACGGGAGATCCTTGAG -3' and 5'-GTGCGGCCGCTCCTTTGACTCCACCTTTGG -3' were used to clone *taperin* fragment into pEGFP-N3 vector. Plasmids were then sequenced using CMV-forward primer (5'-CGCAAATGGGCGGTAGGCGTG-3').

Scanning Electron Microscopy

The experiments were performed as described (Li et al., 2021; Liu et al., 2018). In brief, inner ears were dissected and fixed at room temperature in HBSS containing 2.5% glutaraldehyde and 4% PFA for 1 hour. The stria vascularis, Reissner's membrane and tectorial membrane were then removed. Post-fixation of samples was performed by immersing them in the same fixative at 4°C for 1 day. Following 1 hour of fixation in 1% OsO_4, samples were serially dehydrated in ethanol, dried in a critical point drier (Autosamdri-815A, Tousimis), finely dissected, and mounted on aluminum stubs. Then, samples were coated with gold and viewed using a JEOL 7800F scanning electron microscope. At least three animals were analyzed for each experimental paradigm.

Auditory Brainstem Response Measurement

Auditory brainstem responses (ABRs) of mice were measured using the TDT Bioacoustic system 3 and the BioSigRZ software as described (Liu et al., 2018). In brief, after mice were anesthetized, electrodes were inserted under the skin at the vertex and ipsilateral ear,

while a ground was inserted near the tail. The speaker was positioned 5 cm away from the mouse ear. Tone stimulus was presented 21 times per second. The averaging window was 10 ms. At each frequency and level combination, an average of 512 responses were calculated. The sound stimulus intensity was started at 90 dB sound pressure level (SPL) and gradually decreased to a sub-threshold level in steps of 10 dB SPL. The ABR thresholds for a range of frequencies (4-28 kHz) were analyzed. If no ABR wave was detected during stimulation at maximum intensity, a nominal threshold of 90 dB was assigned.

Quantification and Statistical Analysis

Kolmogorov-Smirnov test was used to determine the normality of the data distribution. Then Student's two-tailed unpaired t test was used to compare the click ABR thresholds in wild-type and mutant mice (*, $p<0.05$, **, $p<0.01$, ***, $p<0.001$). The two-way ANOVA was used to determine whether the differences of pure-tone thresholds between wild-type and mutant mice were statistically significant. The Bonferroni *post hoc* test was used to determine whether the differences between wild-type and mutant mice were statistically significant in each frequency (*, $p<0.05$, **, $p<0.01$, ***, $p<0.001$).

RESULTS:

Generation of two novel *taperin* mutant mice

Taperin has four exons (Fig. 1A). All identified mutations associated with human deafness are located in exon 1, indicating that it encodes a region required for taperin function (Li et al., 2010; Rehman et al., 2010). According to earlier study, *taperin* most likely has two translation start codons (Rehman et al., 2010). Apart from the first start codon, the 'ATG' sequence between nucleotides 184-186 in human *taperin* and 193-195 in mouse *taperin* represents another possible translational start site (Rehman et al., 2010) (Fig. 1A). Thus, two short guide RNAs (sgRNAs) were designed to generate *taperin* mutants. The first sgRNA is specific for the region immediately after the first start codon, whereas the second sgRNA is specific for the region following the second start codon. We genotyped 73 mice of F0 generation and found that only the first sgRNA resulted in genomic editing. Finally, we generated several distinct mouse lines, one of which contains a 103-bp nucleotide insertion between nucleotide 217 and 218 in exon 1 of *taperin* (referred to previously as $taperin^{In103/In103}$) (Liu et al., 2018). Additionally, we obtained two additional *taperin* mutant mice, one with a 23-bp deletion from nucleotide 106 to 128 (referred to as $taperin^{D23/D23}$ hereafter) and another with an 11-bp deletion from nucleotide 118-128 (referred to as $taperin^{D11/D11}$ hereafter) (Fig. 1A and Supplemental Fig. 1). Due to the frameshifts generated by these indels, early stop codons are created following the first start codon (Fig. 1A).

Next, whole mount immunostaining was performed to evaluate whether these mice lack taperin, using a commercial antibody against amino acids 447-512, encoded by exon 1 of *taperin* (Fig. 1B) (Liu et al., 2018; Rehman et al., 2010). Immunostaining signal of taperin was robust at the base of stereocilia in wild-type hair cells, but not in hair cells dissected from $taperin^{In103/In103}$ mice at the age of postnatal day 5 (P5) (Fig. 1C), suggesting that the 103-bp insertion not only generates an early stop codon following the first translation

start codon, but also dramatically increases the distance between the second start codon and the ribosomal recruiting site, effectively eliminating protein translation from the second start codon. Interestingly, the intensity of staining was dramatically reduced, but not eliminated, in *taperin*$^{D23/D23}$ and *taperin*$^{D11/D11}$ mice, implying the production of a truncated taperin that could be translated via the second start codon (Fig. 1C). Notably, the signal at the kinocilium region is non-specific in wild-type and *taperin* mutant hair cells (Fig. 1C), as we previously observed no localization of exogenously expressed taperin in kinocilium (Liu et al., 2018). Additionally, we raised a new antibody against amino acids 730-749, encoded by exon 4 of *taperin* (Fig. 1B). Taperin immunostaining was concentrated at the base of stereocilia, without any signal in the kinocilium of wild-type mice. No signal was obtained in *taperin*$^{In103/In103}$ hair cells, whereas weak immunostaining signal was observed at the base of stereocilia in *taperin*$^{D23/D23}$ and *taperin*$^{D11/D11}$ hair cells (Fig. 1D-1G). These results suggest that *taperin*$^{D23/D23}$ and *taperin*$^{D11/D11}$ mice indeed express a truncated taperin with a low level of expression.

Progressive hearing loss in *taperin* mutant mice

To characterize the auditory function of these mice, we measured ABRs to broadband click or pure tone stimuli. At the age of 2 months, *taperin*$^{D23/D23}$ and *taperin*$^{D11/D11}$ mice had elevated hearing thresholds while *taperin*$^{In103/In103}$ mice had profound hearing loss (Fig. 2A). By the age of 6 months, *taperin*$^{D23/D23}$ and *taperin*$^{D11/D11}$ mice were profoundly deaf (Fig. 2B). These results suggest that the truncated protein expressed in *taperin*$^{D23/D23}$ and *taperin*$^{D11/D11}$ mice retains some functionals properties.

Reducing taperin expression corrects morphological defects of stereocilia in *Grxcr2* null hair cells

GRXCR2 interacts with taperin (Liu et al., 2018). *Grxcr2* null mutant mice (referred to as *Grxcr2*$^{-/-}$ mice hereafter) have disorganized stereocilia, resulting in profound hearing loss. We crossed *Grxcr2*$^{-/-}$ mice with *taperin*$^{In103/In103}$ mice in our previous studies. Interestingly, the stereocilia morphological defects were corrected in *Grxcr2*$^{-/-}$*taperin*$^{In103/+}$ and *Grxcr2*$^{-/-}$*taperin*$^{In103/In103}$ mice, suggesting that decreasing taperin expression could correct morphological defects in *Grxcr2*$^{-/-}$ hair cells (Liu et al., 2018). To corroborate this finding, we crossed *taperin*$^{D23/D23}$ with *Grxcr2*$^{-/-}$ mice. Phalloidin staining of whole-mounted P7 sensory epithelia from wild-type mice revealed three rows of outer hair cells and one row of inner hair cells that were well organized, with a strong immunostaining signal of GRXCR2 at the base (Fig. 3A). Consistent with previous observations (Avenarius et al., 2018; Liu et al., 2018), stereocilia were severely disorganized in *Grxcr2*$^{-/-}$ hair cells (Fig. 3A). Remarkably, bundle morphology was largely normal in *Grxcr2*$^{-/-}$ *taperin*$^{D23/+}$ and *Grxcr2*$^{-/-}$*taperin*$^{D23/D23}$ mice, despite the absence of GRXCR2 signal in hair cells (Fig. 3A and supplemental Fig. 2). Additionally, *Grxcr2*$^{-/-}$*taperin*$^{D23/+}$ and *Grxcr2*$^{-/-}$*taperin*$^{D23/D23}$ mice retain well-organized stereocilia at 3 months of age (Fig. 3B). Notably, taperin immunostaining signal was significantly lower in *Grxcr2*$^{-/-}$*taperin*$^{D23/+}$ hair cells compared to wild-type hair cells. We detected no residual taperin immunostaining signal in adult *Grxcr2*$^{-/-}$*taperin*$^{D23/D23}$ hair cells, which may be due to the low stability of the truncated taperin protein (Fig. 3B and 3C).

Scanning electron microscopy was then performed to analyze the stereociliary structure in more detail. Consistent with fluorescence microscopy, both *Grxcr2*$^{-/-}$ *taperin*$^{D23/+}$ and *Grxcr2*$^{-/-}$ *taperin*$^{D23/D23}$ hair cells exhibited well-organized hair bundles (Fig. 4). These results suggest that reducing taperin expression indeed recovers stereocilia morphological abnormalities in *Grxcr2*$^{-/-}$ mice.

Reducing taperin expression restores hearing in *Grxcr2* null mice

Then we sought to determine whether reducing taperin expression restores hearing in *Grxcr2* null mutants. The ABRs to click stimuli and pure tones were measured in 6-week-old mice with *Grxcr2*$^{-/-}$, *Grxcr2*$^{-/-}$ *taperin*$^{D23/+}$ and *Grxcr2*$^{-/-}$ *taperin*$^{D23/D23}$ genotypes. Consistent with the morphological results, the hearing threshold for click stimuli was reduced to ~40 dB sound pressure level (SPL) in *Grxcr2*$^{-/-}$ *taperin*$^{D23/+}$ mice (Fig. 5A). The pure tone thresholds were also significantly reduced, particularly at lower frequencies. Although *Grxcr2*$^{-/-}$ *taperin*$^{D23/D23}$ mice have relatively normal stereocilia, they exhibited profound hearing loss across all frequencies examined, ranging from 4 to 28 kHz (Fig. 5B). Additionally, we measured the hearing thresholds of mice at 3 months of age. In *Grxcr2*$^{-/-}$ *taperin*$^{D23/+}$ mice, the hearing threshold for click stimuli was around 50 dB SPL (Fig. 5C). ABR of pure tones reveals that 3-month-old *Grxcr2*$^{-/-}$ *taperin*$^{D23/+}$ mice still had significantly lower hearing thresholds, particularly at lower frequencies, than *Grxcr2*$^{-/-}$ *taperin*$^{D23/D23}$ mice, which had profound hearing loss across the entire analyzed frequency spectrum (Fig. 5D). These findings confirmed that reducing taperin expression partially restores hearing in *Grxcr2* null mice.

DISCUSSION:

Mutations of GRXCR2 are associated with hearing loss in humans (Imtiaz et al., 2014; Wonkam et al., 2021). The pathological mechanisms are still not very clear. We previously discovered that GRXCR2 is required for the correct localization of taperin at the base of stereocilia and that reducing taperin expression restores the hearing loss caused by GRXCR2 loss (Liu et al., 2018). We generated two novel *taperin* mutant mice in this study and confirmed that reducing taperin expression indeed corrects the morphological defects of stereocilia and partially restores hearing in *Grxcr2* null mice.

We detected a residual immunostaining signal for taperin in *taperin*$^{D11/D11}$ and *taperin*$^{D23/D23}$ mice, indicating that deletion of a short sequence at the N terminus does not fully eliminate taperin expression. Consistently, the phenotype of *taperin*$^{D11/D11}$ and *taperin*$^{D23/D23}$ mice exhibit a milder phenotype than *taperin*$^{In103/In103}$ mice, in which the 103-bp insertion effectively eliminating protein translation. In agreement with this, *taperin* mutant mice with a 1-bp or 43-bp deletion in the same region of the genome also exhibit mild phenotypes (Men et al., 2019). Further study into different taperin isoforms and their expression profiles in wild-type and *taperin*$^{D23/D23}$ mice will be of interest. The results in this study also show that *Grxcr2*$^{-/-}$ *taperin*$^{D23/D23}$ mice have profound hearing loss at 6 weeks of age, whereas *taperin*$^{D23/D23}$ mice have residual hearing, suggesting that GRXCR2 has additional functions in addition to determining the taperin's localization. In line with that, we reported that GRXCR2 interacts with CLIC5, another protein associated with

hearing loss that is located at the base of stereocilia. Disrupting the interaction between GRXCR2 with CLIC5 has a negligible effect on stereocilia morphogenesis but results in moderate low-frequency hearing loss and severe high-frequency hearing loss (Li et al., 2021). These findings suggest that the interaction between GRXCR2 and CLIC5 may play a role in the hearing loss observed in *Grxcr2*$^{-/-}$*taperin*$^{D23/D23}$ mice. Besides the interaction with CLIC5, GRXCR2 may interact with other unidentified proteins which are also required for normal hearing. Screening novel interacting proteins of GRXCR2 and investigating the extent to which those binding partners are required for auditory perception will be informative.

In summary, this study confirms that reducing taperin expression does indeed correct stereocilia morphological abnormalities and partially restore hearing in *Grxcr2* null mice.

Supplementary Material

Refer to Web version on PubMed Central for supplementary material.

ACKNOWLEDGMENTS

This work was supported by National Institute on Deafness and Other Communication Disorders (NIDCD) grant DC017147 (B. Z.) and Indiana University School of Medicine startup funding (B. Z.).

REFERENCES

Avenarius MR, Jung JY, Askew C, Jones SM, Hunker KL, Azaiez H, Rehman AU, Schraders M, et al. (2018), Grxcr2 is required for stereocilia morphogenesis in the cochlea. PLoS One 13:e0201713. [PubMed: 30157177]

Barr-Gillespie PG (2015), Assembly of hair bundles, an amazing problem for cell biology. Mol Biol Cell 26:2727–2732. [PubMed: 26229154]

Drummond MC, Barzik M, Bird JE, Zhang DS, Lechene CP, Corey DP, Cunningham LL, Friedman TB (2015), Live-cell imaging of actin dynamics reveals mechanisms of stereocilia length regulation in the inner ear. Nat Commun 6:6873. [PubMed: 25898120]

Imtiaz A, Kohrman DC, Naz S (2014), A frameshift mutation in GRXCR2 causes recessively inherited hearing loss. Hum Mutat 35:618–624. [PubMed: 24619944]

Kitajiri S, Sakamoto T, Belyantseva IA, Goodyear RJ, Stepanyan R, Fujiwara I, Bird JE, Riazuddin S, et al. (2010), Actin-bundling protein TRIOBP forms resilient rootlets of hair cell stereocilia essential for hearing. Cell 141:786–798. [PubMed: 20510926]

Li J, Liu C, Zhao B (2021), N-Terminus of GRXCR2 Interacts With CLIC5 and Is Essential for Auditory Perception. Front Cell Dev Biol 9:671364. [PubMed: 34026762]

Li Y, Pohl E, Boulouiz R, Schraders M, Nurnberg G, Charif M, Admiraal RJ, von Ameln S, et al. (2010), Mutations in TPRN cause a progressive form of autosomal-recessive nonsyndromic hearing loss. Am J Hum Genet 86:479–484. [PubMed: 20170898]

Liu C, Luo N, Tung CY, Perrin BJ, Zhao B (2018), GRXCR2 Regulates Taperin Localization Critical for Stereocilia Morphology and Hearing. Cell Rep 25:1268–1280 e1264. [PubMed: 30380417]

Men Y, Li X, Tu H, Zhang A, Fu X, Wang Z, Jin Y, Hou C, et al. (2019), Tprn is essential for the integrity of stereociliary rootlet in cochlear hair cells in mice. Front Med 13:690–704. [PubMed: 30159668]

Narayanan P, Chatterton P, Ikeda A, Ikeda S, Corey DP, Ervasti JM, Perrin BJ (2015), Length regulation of mechanosensitive stereocilia depends on very slow actin dynamics and filament severing proteins. Nat Commun 6:6855. [PubMed: 25897778]

Olusanya BO, Davis AC, Hoffman HJ (2019), Hearing loss: rising prevalence and impact. Bull World Health Organ 97:646–646A. [PubMed: 31656325]

Rehman AU, Morell RJ, Belyantseva IA, Khan SY, Boger ET, Shahzad M, Ahmed ZM, Riazuddin S, et al. (2010), Targeted capture and next-generation sequencing identifies C9orf75, encoding taperin, as the mutated gene in nonsyndromic deafness DFNB79. Am J Hum Genet 86:378–388. [PubMed: 20170899]

Shearer AE, Hildebrand MS, Smith RJH (1993) Hereditary Hearing Loss and Deafness Overview. In: GeneReviews((R)), vol. (Adam MP, Ardinger HH, Pagon RA, Wallace SE, Bean LJH, Gripp KW, Mirzaa GM, et al., eds). Seattle (WA).

Wonkam A, Lebeko K, Mowla S, Noubiap JJ, Chong M, Pare G (2021), Whole exome sequencing reveals a biallelic frameshift mutation in GRXCR2 in hearing impairment in Cameroon. Mol Genet Genomic Med 9:e1609. [PubMed: 33528103]

Yang H, Wang H, Jaenisch R (2014), Generating genetically modified mice using CRISPR/Cas-mediated genome engineering. Nat Protoc 9:1956–1968. [PubMed: 25058643]

Zhao B, Muller U (2015), The elusive mechanotransduction machinery of hair cells. Curr Opin Neurobiol 34:172–179. [PubMed: 26342686]

Taperin is required for hearing.

Reducing taperin expression corrects stereocilia defects in *Grxcr2* null mice.

Reducing taperin expression partially restores the hearing in *Grxcr2* null mice.

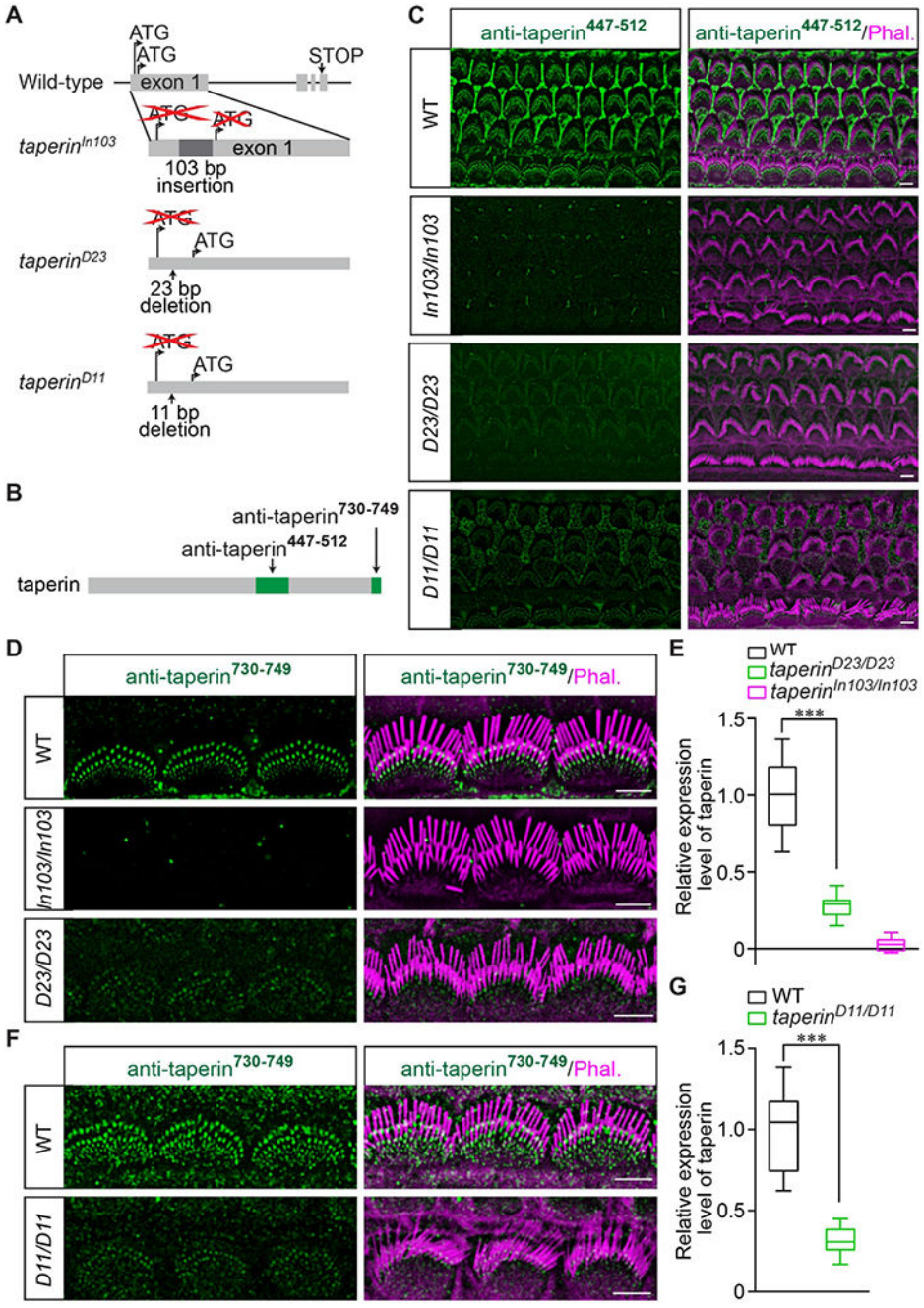

Figure 1: Generation of *taperin* mutant mice.

(A) Diagram of the strategy to generate *taperin* mutant mice by using CRISPR/Cas9 system. Two potential translation start codons ('ATG') of *taperin* are indicated in the diagram. Two sgRNAs were designed to target regions after two start codons respectively. Three mouse lines with 103-bp insertion, 23-bp deletion or 11-bp deletion were generated. **(B)** A commercial antibody purchased from MilliporeSigma recognizes amino acids 447-512, which are encoded by exon 1 of *taperin*. The self-raised antibody recognizes amino acids 730-749, which are encoded by exon 4 of *taperin*. **(C)** Cochlear whole mounts

from wild-type mice, *taperin*$^{In103/In103}$, *taperin*$^{D23/D23}$ and *taperin*$^{D11/D11}$ mice at P5 of age were stained for taperin (green) using antibody against amino acids 447-512, and phalloidin (magenta) to indicate the stereocilia. Note, the intensity of taperin was reduced but not abolished in *taperin*$^{D23/D23}$ or *taperin*$^{D11/D11}$ mice. No staining at the base of stereocilia as well as supporting cells in *taperin*$^{In103/In103}$ mice. The weak residual immunoreactivity at kinocilium in wild-type and *taperin* mutants was caused by nonspecific antibody binding. **(D)** Cochlear whole mounts dissected from P7 wild-type, *taperin*$^{In103/In103}$ and *taperin*$^{D23/D23}$ mice were stained using antibody against amino acids 730-749 of taperin. (**E**) Quantification of taperin expression level in P7 wild-type, *taperin*$^{In103/In103}$ and *taperin*$^{D23/D23}$ mice, as shown in (D). Box-and-whiskers plots include the median of the data (represented by the horizontal bar across the box), the 25th and 75th percentiles of the distribution (represented by the bottom and top lines of the box, respectively), and the 5th and 95th percentiles of the distribution (represented by the bottom and top whiskers, respectively). Two-tailed unpaired t test was used to compare the difference between wild-type and *taperin*$^{D23/D23}$ hair cells: ***$p < 0.001$, $t(82) = 20.13$. (**F**) Cochlear whole mounts dissected from P4 wild-type and *taperin*$^{D11/D11}$ mice were stained using antibody against amino acids 730-749 of taperin. (**G**) Quantification of taperin expression level in P4 wild-type and *taperin*$^{D11/D11}$ mice, as shown in (F). Box-and-whiskers plots include the median of the data (represented by the horizontal bar across the box), the 25th and 75th percentiles of the distribution (represented by the bottom and top lines of the box, respectively), and the 5th and 95th percentiles of the distribution (represented by the bottom and top whiskers, respectively). Two-tailed unpaired t test was used to compare the difference between wild-type and *taperin*$^{D11/D11}$ hair cells: ***$p < 0.001$, $t(103) = 19.25$. Scale bars: 5 μm.

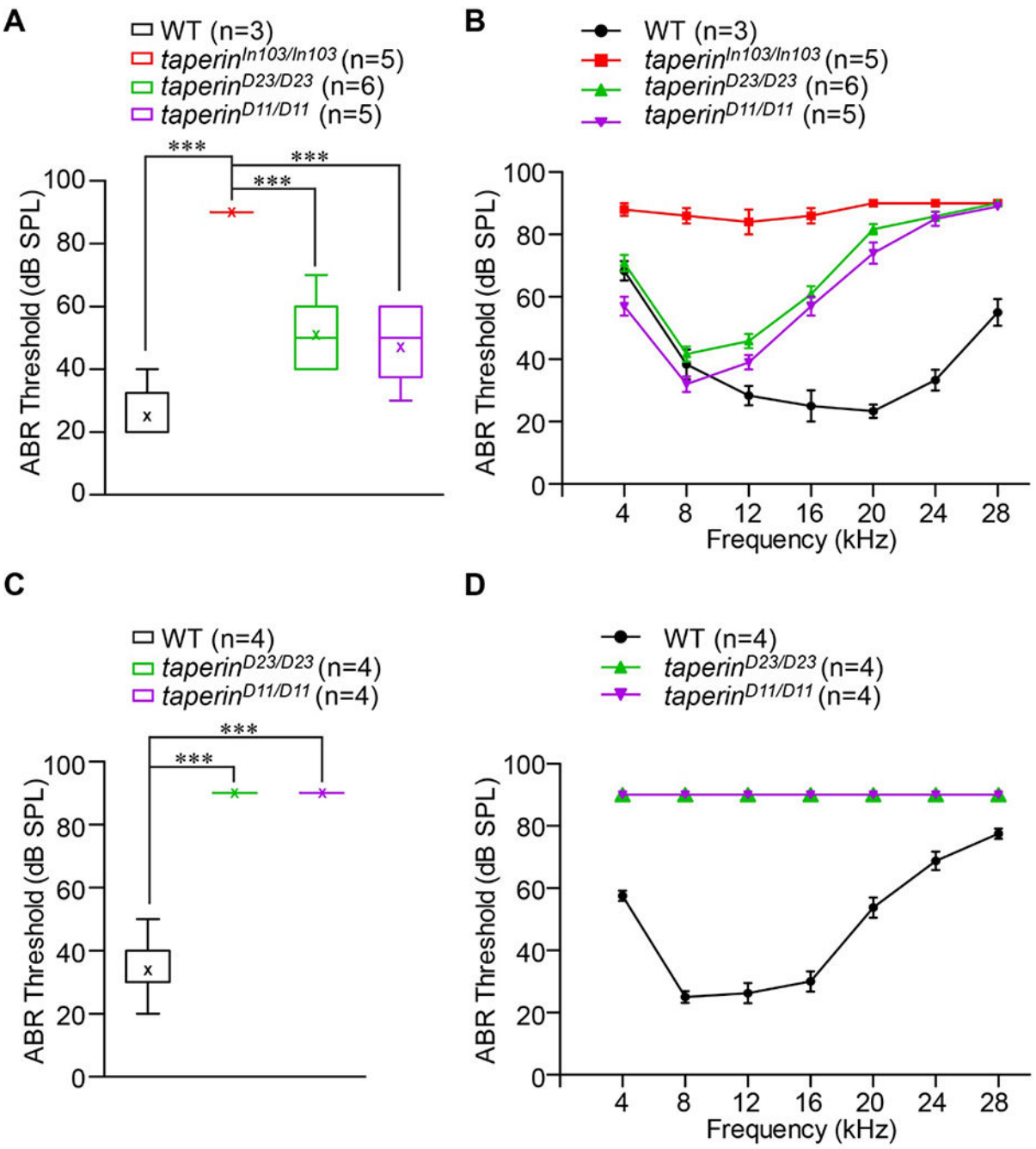

Figure 2: Progressive hearing loss in *taperin*$^{D23/D23}$ and *taperin*$^{D11/D11}$ mice.

(A-B) ABR thresholds for click stimuli (A) and pure tones (B) in wild-type, *taperin*$^{In103/In103}$, *taperin*$^{D23/D23}$ and *taperin*$^{D11/D11}$ mice at 2 months of age. **(C-D)** ABR thresholds for click stimuli (C) and pure tones (D) in wild-type, *taperin*$^{D23/D23}$ and *taperin*$^{D11/D11}$ mice at 6 months of age. The numbers of analyzed mice are indicated. Each mouse had either one or both ears measured. Box-and-whiskers plots in (A) and (C) include the mean of the data (represented by "X"), the median of the data (represented by the horizontal bar across the box), the 25th and 75th percentiles of the distribution (represented

by the bottom and top lines of the box, respectively), and the 5th and 95th percentiles of the distribution (represented by the bottom and top whiskers, respectively). Two-tailed unpaired t test was used in (A) and (C): 2-month-old wild-type vs. *taperin*$^{In103/In103}$ mice, ***p < 0.001, t (9) = 17.22; 2-month-old *taperin*$^{In103/In103}$ vs. *taperin*$^{D23/D23}$ mice, ***p < 0.001, t (15) = 7.933; 2-month-old *taperin*$^{In103/In103}$ vs. *taperin*$^{D23/D23}$ mice, ***p < 0.001, t (13) = 8.141; 6-month-old wild-type vs. *taperin*$^{D23/D23}$ mice, ***p < 0.001, t (14) = 17.37; 6-month-old wild-type vs. *taperin*$^{D11/D11}$ mice, ***p < 0.001, t (14) = 17.37. Data in (B) and (D) are shown as the mean ± standard error of the mean (SE). Two-way ANOVA was used in (B) and (D): 2-month-old wild-type vs. *taperin*$^{In103/In103}$ mice, p < 0.001, F (1, 72) = 718.96; 2-month-old wild-type vs. *taperin*$^{D23/D23}$ mice, p < 0.001, F (1, 128) = 430.37; 2-month-old wild-type vs. *taperin*$^{D11/D11}$ mice, p < 0.001, F (1, 112) = 221.84; 2-month-old *taperin*$^{In103/In103}$ vs. *taperin*$^{D23/D23}$ mice, p < 0.001, F (1, 120) = 219.93; 2-month-old *taperin*$^{In103/In103}$ vs. *taperin*$^{D11/D11}$ mice, p < 0.001, F (1, 104) = 290.32; 6-month-old wild-type vs. *taperin*$^{D23/D23}$ mice, p < 0.001, F (1, 112) = 1719.56; 6-month-old wild-type vs. *taperin*$^{D11/D11}$ mice, p < 0.001, F (1, 112) = 1719.56.

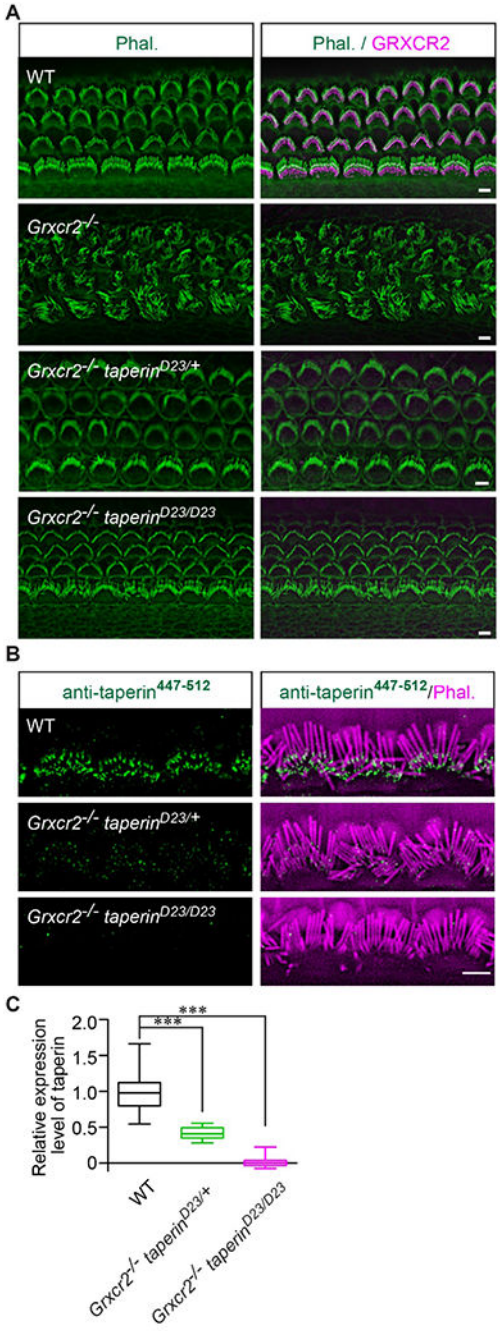

Figure 3: Analysis of hair bundle morphology by fluorescence microscopy.

(A) Cochlear whole mounts from P7 wild-type, *Grxcr2*$^{-/-}$, *Grxcr2*$^{-/-}$ *taperin*$^{D23/+}$, and *Grxcr2*$^{-/-}$ *taperin*$^{D23/D23}$ mice were stained for phalloidin (green) and GRXCR2 (magenta). Note, relatively normal stereocilia bundles in *Grxcr2*$^{-/-}$ *taperin*$^{D23/+}$ and *Grxcr2*$^{-/-}$ *taperin*$^{D23/D23}$ mice. **(B)** Cochlear whole mounts from 3-month-old wild-type, *Grxcr2*$^{-/-}$ *taperin*$^{D23/+}$, and *Grxcr2*$^{-/-}$ *taperin*$^{D23/D23}$ mice were stained for taperin (green) and phalloidin (magenta). **(C)** Quantification of taperin expression level as shown in (B). Box-and-whiskers plots include the median of the data (represented by the horizontal bar

across the box), the 25th and 75th percentiles of the distribution (represented by the bottom and top lines of the box, respectively), and the 5th and 95th percentiles of the distribution (represented by the bottom and top whiskers, respectively). Two-tailed unpaired t test was used to compare: wild-type and *Grxcr2*$^{-/-}$ *taperin*$^{D23/+}$ hair cells, ***p < 0.001, t (137) = 15.82; wild-type and *Grxcr2*$^{-/-}$ *taperin*$^{D23/D23}$ hair cells, ***p < 0.001, t (133) = 25.76. Scale bars: 5 μm.

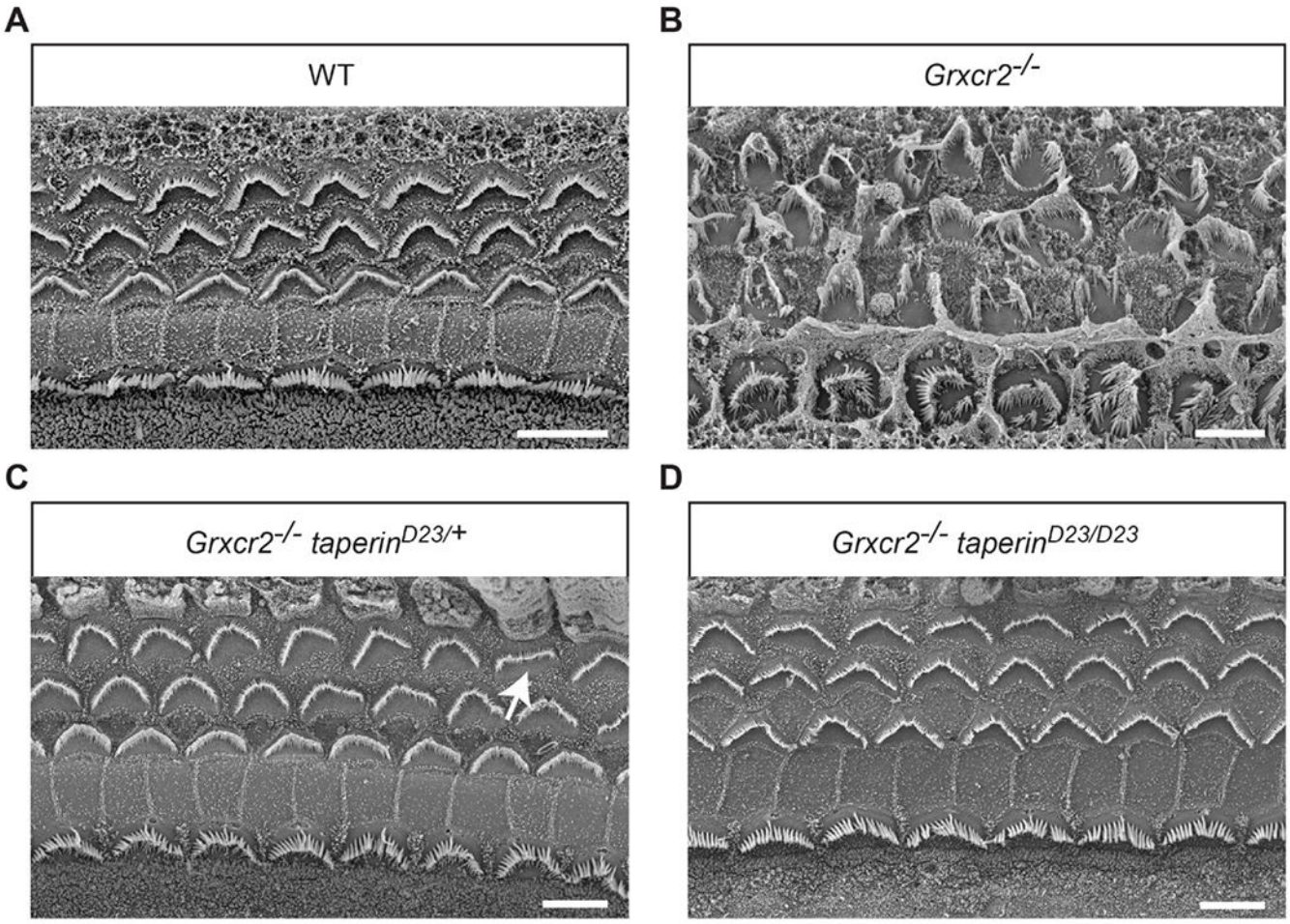

Figure 4: Analysis of hair bundle morphology by scanning electron microscopy.

Cochlear epithelia from P7 wild-type (A), *Grxcr2*$^{-/-}$ (B), *Grxcr2*$^{-/-}$ *taperin*$^{D23/+}$ (C), and *Grxcr2*$^{-/-}$ *taperin*$^{D23/D23}$ (D) mice were analyzed by scanning electron microscopy. Note, relatively normal stereocilia bundles in *Grxcr2*$^{-/-}$ *taperin*$^{D23/+}$ and *Grxcr2*$^{-/-}$ *taperin*$^{D23/D23}$ mice. A few outer hair cells (arrow) in *Grxcr2*$^{-/-}$ *taperin*$^{D23/+}$ mice exhibited disorganized stereocilia. Scale bars: 5 μm.

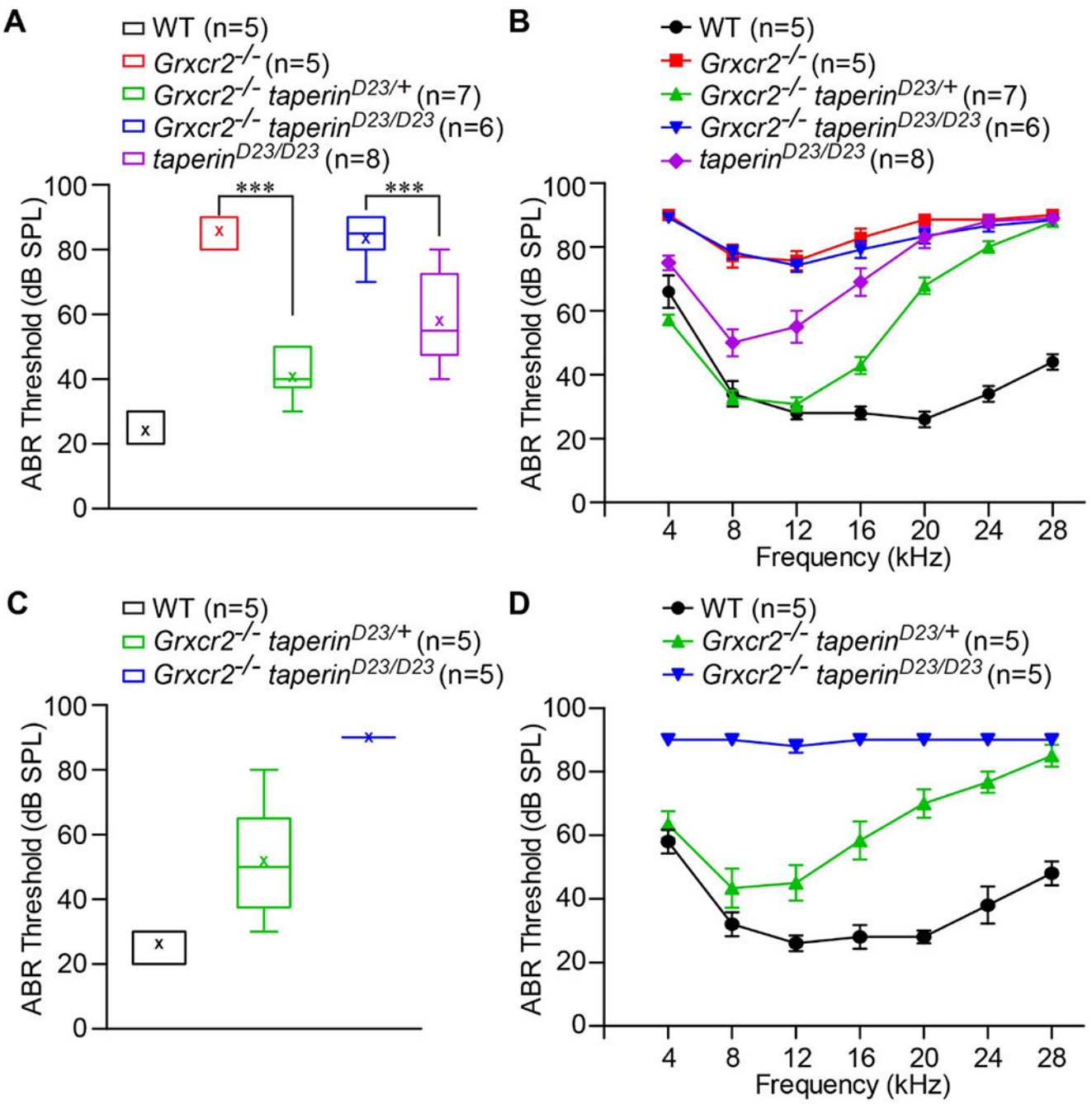

Figure 5: Analysis of hearing function by ABR.

(**A-B**) ABR thresholds for click stimuli (**A**) and pure tones (**B**) at 6 weeks of age. The numbers of analyzed mice are indicated. Results are represented as mean ± SE. ***p < 0.001 by Student's t test (A). P < 0.001 between *Grxcr2*$^{-/-}$ and *Grxcr2*$^{-/-}$ *taperin*$^{D23/+}$ mice, and between *taperin*$^{D23/D23}$ and *Grxcr2*$^{-/-}$ *taperin*$^{D23/D23}$ mice by two-way ANOVA (B). (**C-D**) ABR thresholds for click stimuli (**C**) and pure tones (**D**) at 3 months of age. The numbers of analyzed mice are indicated. Each mouse had either one or both ears measured. Box-and-whiskers plots in (A) and (C) include the mean of the data (represented by "X"),

the median of the data (represented by the horizontal bar across the box), the 25th and 75th percentiles of the distribution (represented by the bottom and top lines of the box, respectively), and the 5th and 95th percentiles of the distribution (represented by the bottom and top whiskers, respectively). Two-tailed unpaired t test was used in (A) and (C): 6-week-old wild-type vs. *Grxcr2*$^{-/-}$ mice, ***p < 0.001, t (10) = 19.52; 6-week-old *Grxcr2*$^{-/-}$ vs. *Grxcr2*$^{-/-}$*taperin*$^{D23/+}$ mice, ***p < 0.001, t (19) = 14.41; 6-week-old *Grxcr2*$^{-/-}$*taperin*$^{D23/+}$ vs. *Grxcr2*$^{-/-}$*taperin*$^{D23/D23}$ mice, ***p < 0.001, t (20) = 5.163; 6-week-old wild-type vs. *Grxcr2*$^{-/-}$*taperin*$^{D23/+}$ mice, ***p < 0.001, t (17) = 4.640; 6-week-old wild-type vs. *taperin*$^{D23/D23}$ mice, ***p < 0.001, t (13) = 4.907; 3-month-old *Grxcr2*$^{-/-}$*taperin*$^{D23/+}$ vs. *Grxcr2*$^{-/-}$*taperin*$^{D23/D23}$ mice, ***p < 0.001, t (9) = 4.934. Data in (B) and (D) are shown as the mean ± standard error of the mean (SE). Two-way ANOVA was used in (B) and (D): 6-week-old wild-type vs. *Grxcr2*$^{-/-}$ mice, p < 0.001, F (1, 80) = 1161.98; 6-week-old *Grxcr2*$^{-/-}$ vs. *Grxcr2*$^{-/-}$*taperin*$^{D23/+}$ mice, p < 0.001, F (1, 152) = 471.25; 6-week-old *Grxcr2*$^{-/-}$*taperin*$^{D23/+}$ vs. *Grxcr2*$^{-/-}$*taperin*$^{D23/D23}$ mice, p < 0.001, F (1, 160) = 49.77; 6-week-old wild-type vs. *taperin*$^{D23/D23}$ mice, p < 0.001, F (1, 104) = 357.90; 3-month-old *Grxcr2*$^{-/-}$*taperin*$^{D23/+}$ vs. *Grxcr2*$^{-/-}$*taperin*$^{D23/D23}$ mice, p < 0.001, F (1, 72) = 168.31.